Oil Shale, 2025, Vol. 42, No. 2, pp. 167–180
doi: https://doi.org/10.3176/oil.2025.2.02 ISSN 0208-189X

Pyrolysis characteristics of Maoming oil shale using visual reactor in the presence of supercritical water

Tian Xie[(a)]*, Hai Huang[(a)], Yi Zhang[(a)], Zhiguo Wang[(a,c)], Shuai Li[(a)], Zilong Zeng[(a)], Hui Jin[(b)], Yechun Wang[(b)], Qiuyang Zhao[(b)]*

(a) Xi'an Shiyou University, Xi'an 710065, China
(b) State Key Laboratory of Multiphase Flow in Power Engineering, Xi'an Jiaotong University, Xi'an 710049, China
(c) Engineering Research Center of Smart Energy and Carbon Neutral in Oil & Gas Field, Universities of Shaanxi Province, Xi'an 710065, China

Received 16 October 2024, accepted 9 April 2025, available online 11 April 2025

Abstract. *This study introduces a novel visual online observation technique for identifying the critical temperature for oil generation. It also examines the hydrocarbon generation properties of Maoming oil shale when subjected to supercritical water. Findings indicate that the critical temperature for Maoming oil shale in supercritical water ranges from 262 to 292 °C, and the visualization reactor facilitates the investigation of this critical temperature. The organic carbon conversion rate for Maoming oil shale can exceed 25.4% within a limited reaction time of one hour. Increasing the water-shale mass ratio enhances the overall conversion of organic carbon in the oil shale and boosts oil production, although it does not significantly improve gas production. Additionally, a higher water-shale mass ratio can decrease the heavy oil fraction in the oil and enhance the selectivity for hydrogen and methane in the gas produced.*

Keywords: *oil shale, supercritical water, conversion, visualization.*

1. Introduction

Unconventional oil and gas resources are highly regarded, with oil shale being a significant type. As a source rock, it has considerable potential for hydrocarbon generation, with nearly all its organic matter existing in solid form. Without human intervention, this solid organic matter would take thousands of years to evolve into fluid hydrocarbons under natural underground temperature and pressure [1]. However, due to the current global energy crisis, there is

* Corresponding authors, xietian@xsyu.edu.cn, qyzhao@mail.xjtu.edu.cn

a pressing need to find methods to speed up the conversion of solid organic matter into hydrocarbons, so that these resources can contribute to energy supply necessary for societal development.

Initially, the method for utilizing oil shale resources involved transporting the ore to a retort and subjecting it to high temperatures to extract oil and gas. However, this approach has been found to be inefficient and produces significant pollution [2]. While this surface conversion method still holds some economic value for certain outcrop oil shale deposits, it is less effective for deeper deposits. In such cases, the oil shale must be mined using techniques similar to coal mining, which leads to considerable waste of labor, materials, and financial resources. Consequently, there has been a shift towards underground in situ conversion methods to produce oil and gas directly in place, utilizing technologies such as electric heating, fluid heating, radiation heating, and combustion heating. Each of these methods can convert kerogen in oil shale into oil and gas to varying extents. However, they also have their drawbacks, including the lengthy process of electric heating, challenges in miniaturizing radiation heating equipment, low energy efficiency in fluid heating, and difficulties in controlling combustion heating [3–8].

In recent years, there has been growing interest in the impressive capabilities of supercritical water for the pyrolysis of large organic molecules [9–13]. As a result, Guo Liejin's team at Xi'an Jiaotong University has applied supercritical water to the in situ conversion of oil shale, developing a technology that utilizes supercritical water to produce hydrocarbons from oil shale [14]. Essentially, this method involves injecting supercritical water as a thermal medium into oil shale reservoirs, allowing it to interact thoroughly with kerogen and subsequently generate oil and gas. The physical properties of supercritical water can vary widely and can be adjusted by changing temperature and pressure, enabling targeted control over the types of hydrocarbon products produced [15]. Compared to existing effective in situ conversion methods using subcritical water and high-temperature steam, supercritical water conversion technology demonstrates significant improvements in energy efficiency [16]. Additionally, supercritical water is capable of transporting substantial amounts of heat, facilitating the rapid conversion of kerogen into hydrocarbons [15].

Experimental equipment for hydrocarbon generation from oil shale in the presence of supercritical water has been widely studied. Currently, there are two primary types of conversion experiments. One utilizes a fully enclosed reactor, which conducts static product tests. While this setup is easy to operate, the cooling stage can affect the product's composition. The other type involves a semi-closed or open device, which, despite its more complex structure and higher cost, allows for the collection of products for testing at any time by opening a valve. The efficiency of hydrocarbon generation from oil shale pyrolysis in a supercritical water environment and the factors influencing it have been thoroughly investigated [17–23]. Key factors affecting hydrocarbon generation include temperature, pressure, water-shale mass ratio, reaction time, and material size. There is an optimal temperature for maximizing hydrocarbon generation efficiency; exceeding this temperature can increase the tendency for polymerization and coking, reducing the utilization rate of organic matter. In a closed reactor, higher pressure can cause the pores in the shale to collapse, decreasing hydrocarbon generation efficiency, though it has minimal impact on product composition. Increasing the water-shale mass ratio tends to lighten the product, and with sufficient reaction time, gas can become the dominant component of the hydrocarbon product. Additionally, the introduction of certain mixed fluids or biomass can either positively or negatively influence the hydrocarbon generation process [17].

In summary, extensive research has been conducted on the mechanisms and laws of hydrocarbon generation from oil shale in supercritical water. Previous studies have identified a critical temperature threshold for the pyrolysis of oil shale, indicating that oil and gas products will not be produced if the temperature is below this threshold. Only when the temperature surpasses the critical point does the oil shale begin to generate oil and gas. Understanding this threshold temperature is crucial for managing and controlling the preheating of reservoir wells. Currently, the primary method for determining the threshold temperature involves using closed or open reactors for isothermal or non-isothermal heating tests at various temperatures, which can be resource-intensive and costly. Therefore, there is a pressing need for a quicker and more cost-effective approach to assess the critical temperature for oil shale generation in specific areas.

The visual non-isothermal heating reaction system developed in this study allows for the determination of the oil generation threshold temperature for a given oil shale in a single experiment, significantly reducing the time needed for this assessment. Additionally, the study explored the impact of the water-shale mass ratio on hydrocarbon generation from Maoming oil shale in the presence of supercritical water. It is hoped that the findings of this research will serve as a valuable reference for advancing the development of oil shale resources.

2. Experimental section

2.1. Experiment system

This study employs a non-isothermal heating reaction system developed independently. The system consists of three main components: an online observation device (including a macro camera and light source), a temperature and pressure monitoring device, and a heating reaction device. The core reactor, which is the central element of the system, is constructed from Hastelloy alloy and has an internal volume of approximately 60 mL. It can reach a maximum temperature of 600 °C and a maximum pressure of 35 MPa.

Sapphire glass visual windows are installed on both the front and back of the reactor, allowing for observation and recording of the entire reaction process inside. The heating rate of this system is set at 4 °C per minute.

2.2. Material

The oil shale used in this experiment originates from the Youganwo Formation in Maoming Basin. It is mainly found in the mining field of the Maoming open pit and the mines of Shigu, Huangtangling, and Yangjiao, among other areas. The remaining deposits are covered by overlying strata (Huangniuling Formation or Quaternary system). The exposed area is about 4 km^2, with the thickness ranging between 19.2–46.5 m. The formation of this group mainly consists of brown-black oil shale with an oil content generally between 5–9%. It includes 1–3 lignite layers in the middle, along with partial clay-rock, fine sandstone and, siltstone. At the bottom, there is a 0.5 m thick conglomerate layer with relatively simple gravel composition, mainly sandstone from the Shangdong Formation. The gravel exhibits poor grinding, is mostly subangular, semi-directionally arranged, and contains coal lines in the middle with poor sorting. Five oil shale samples were used in this experiment, all extracted from the same core (height = 10 cm, radius = 3 cm). Specific information about these samples is presented in Table 1. As shown, Maoming oil shale exhibits strong heterogeneity, especially in terms of microscopic elemental composition.

Table 1. Basic information of Maoming oil shale

Samples	Fischer assay analysis, %			
	Oil	Water	Semicoke	Gas + loss
A-1	8.13	3.99	80.33	7.55
A-2	8.02	3.38	81.22	7.38
A-3	5.12	3.01	84.06	7.81
A-4	7.88	3.22	80.89	8.01
A-5	9.23	4.77	77.78	8.22

Note: Fischer Assay was conducted on an air-dried basis.

2.3. Working conditions and experimental steps

2.3.1. Working conditions

The purpose of this experiment is to find a simple and fast method for determining the critical temperature of oil generation through online visualization of the hydrocarbon generation process of oil shale in a super-critical water atmosphere. In addition, the oil shale from the Maoming

Basin used in this experiment has high water content in the mining site. To preliminarily explore the influence of the water-shale mass ratio on the transformation process, experimental conditions were set as shown in Table 2. The reaction time refers to the time maintained after the temperature reaches the designated working condition temperature.

Table 2. In situ conversion conditions for Maoming oil shale

Experimental type	Temperature, °C	Pressure, MPa	Water-shale mass ratio	Time, h
Visualization	400	25	12:10	1
	400	25	1:1	1
	400	25	1:1	1
	400	25	1:1	1
	400	25	1:1	1

2.3.2. Experimental procedure

The basic experimental procedure has been described in detail in the team's previous research [1]. For the completeness of this study, a brief summary is provided here. First, a certain amount of oil shale and deionized water was added to the reactor. After closing the reactor, leak detection was performed. Once the reactor's tightness was confirmed, the light source and macro camera were turned on, and the visual picture was adjusted to achieve the best view. Next, the heating device was turned on. When the designated reaction time was reached, the heating device was turned off, and the reactor was opened to collect and test the products.

3. Results and discussion

3.1. Visualization of hydrocarbon generation stages in supercritical water for Maoming oil shale

Figure 1 shows selected images of the transformation process of Maoming oil shale in supercritical water. The process mainly includes the following four stages: before the reaction, the appearance of the first visible drop of oil, the gradual miscibility of oil, gas, and water, and the final completely miscible state.

Observation revealed that the temperature range at which the first visible oil drop appeared was 262–292 °C. This range is the critical temperature for oil generation in the supercritical water atmosphere of Maoming oil shale in this experiment. The heating method used was non-isothermal heating. Heating materials were arranged along the inner wall of the heating device housing the visualization reactor. These materials allowed the inner wall temperature to rapidly rise to the design condition temperature, with the time required being almost negligible. During this process, the internal temperature of the visualization reactor slowly raised from room temperature to the designated temperature condition.

It can also be seen from Figure 1 that the whole heating reaction process can be roughly divided into three stages. The first stage was the water vaporization stage, mainly characterized by the gradual vaporization of liquid water with the increase of the temperature. During this stage, no conversion of organic matter occurred.

The second stage was the hydrocarbon generation stage, marked by the conversion of solid organic matter into oil and gas, with oil and gas production gradually increasing. Through the visualization window, the temperature range of visible oil droplets was obtained, representing the critical temperature for oil generation. This temperature range pertained only to oil, which constituted a part of hydrocarbon products.

The critical temperature for the generation of some gas molecules may differ from that of oil, either being lower or higher. This variation largely depended on the structure of the kerogen and the composition of inorganic minerals in the oil shale, because different inorganic minerals could cause different catalytic effects. At the same time, the porosity and permeability of the oil shale also had a certain impact on the process.

The third stage was the miscible–quasi-miscible stage, characterized by the gradual dissolution of the generated oil and gas by supercritical water, forming a quasi-miscible or completely miscible state.

In conclusion, the critical temperature for Maoming oil shale under supercritical water conditions was 262–292 °C, and the visualization reactor created convenient conditions for exploring the critical temperature of oil shale.

Name	Before the reaction	Appearance of the first visible drop of oil	Gradual miscibility of oil, gas, and water	Final completely miscible state
A-1	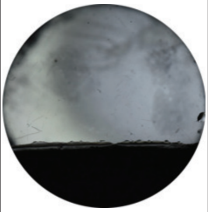 17.66 °C Atmospheric pressure	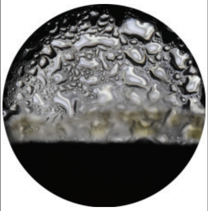 265.43 °C 5.35 MPa	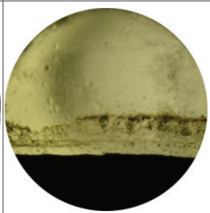 350.40 °C 17.51 MPa	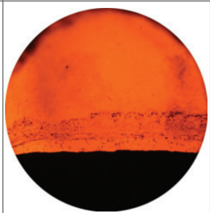 401.33 °C 26.71 MPa

Name	Before the reaction	Appearance of the first visible drop of oil	Gradual miscibility of oil, gas, and water	Final completely miscible state
A-2	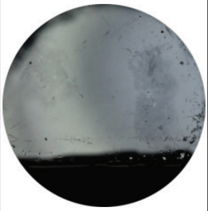 18.23 °C Atmospheric pressure	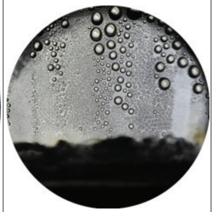 292.01 °C 7.66 MPa	 361.92 °C 19.23 MPa	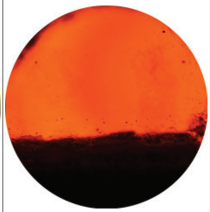 398.00 °C 25.44 MPa
A-3	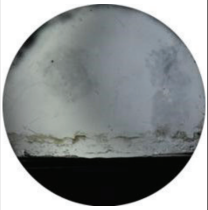 19.37 °C Atmospheric pressure	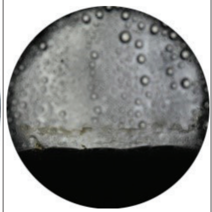 262.39 °C 4.78 MPa	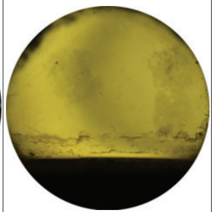 360.00 °C 18.19 MPa	 400.00 °C 24.3 MPa
A-4	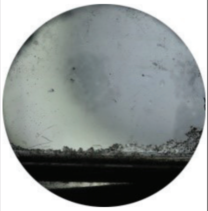 19.81 °C Atmospheric pressure	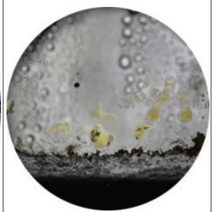 287.36 °C 7.45 MPa	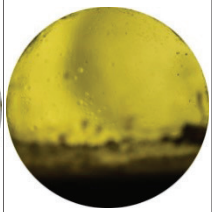 356.86 °C 18.51 MPa	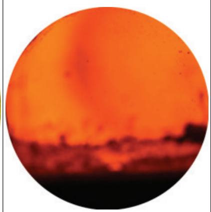 400.37 °C 26.23 MPa
A-5	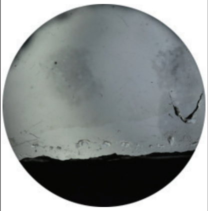 18.90 °C Atmospheric pressure	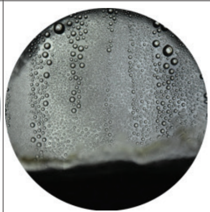 281.94 °C 6.70 MPa	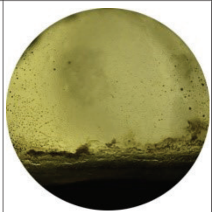 350.00 °C 17.11 MPa	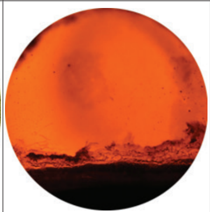 400.00 °C 25.91 MPa

Fig. 1. Visual observation of oil and gas production in Maoming Basin oil shale in the presence of supercritical water.

3.2. Hydrocarbon generation characteristics of Maoming oil shale in the presence of supercritical water

3.2.1. Hydrocarbon generation efficiency

Figures 2–4 show the organic carbon conversion rate, oil production rate, and gas production rate of five oil shale samples from the Maoming Basin under supercritical water conversion. The organic carbon conversion rate is calculated as follows:

$$\text{Organic carbon conversion rate} = \frac{\text{organic carbon mass of the oil shale} - \text{organic carbon mass in the residue}}{\text{organic carbon mass of the oil shale}}$$

It could be seen that supercritical water effectively transformed organic matter from the oil shale of the Paleogene Youguanwo Formation in the Maoming Basin. Under conditions of a temperature of 400 °C, a pressure of 25 MPa, a reaction time of 1 h, and a water-shale mass ratio of 1–1.2, the organic carbon conversion rate exceeded 25.4%, reaching a maximum of 56.4%. The oil production rate reached 2.77 kg oil · t^{-1} shale, while the gas production rate reached 14.6 m^3 gas · t^{-1} shale or more.

According to the designed experimental conditions, the difference between experiment A-1 and the other four experiments lies in the increased water-shale mass ratio, while the working conditions for experiment A-2 to A-5 remain consistent. Based on the results of element testing, although the medium- and low-maturity organic-rich shales used in the five experiments come from the same area, they exhibit strong heterogeneity and significant differences in elemental composition. Therefore, it can be inferred that the final evaluation indexes of the five experiments vary due to internal and external reasons, including the strong heterogeneity of organic-rich shale and the conditions of the exogenous conversion work medium – supercritical water.

Table 3 shows the results of organic carbon content in the wastewater. It can be seen that there is a small amount of organic matter in the wastewater from all five samples, which indicates that the oil shale produces a small amount of soluble organic matter under supercritical water conditions. However, it should be noted that due to the evaporation of some water during the wastewater collection process, the final test results may be inaccurate.

Overall, under the influence of external factors, both the organic carbon conversion rate and the oil production rate showed a certain regular change. An increase in the water-shale mass ratio was conducive to the overall conversion of organic carbon in the oil shale and promoted oil production. However, this increase did not significantly enhance gas production.

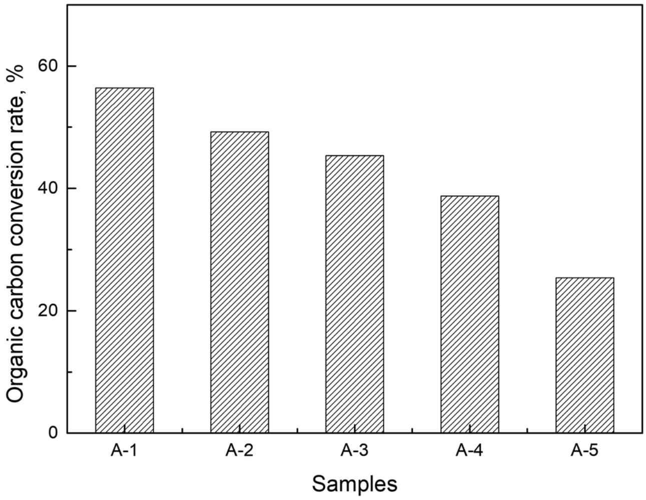

Fig. 2. Organic carbon conversion rate of Maoming oil shale in the presence of supercritical water.

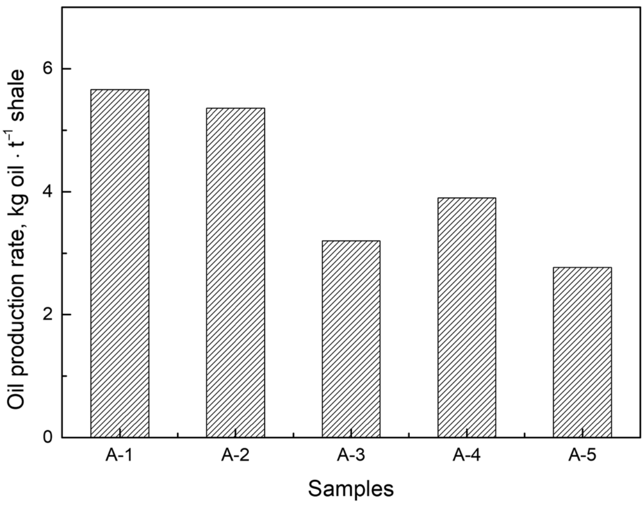

Fig. 3. Oil production rate of Maoming oil shale in the presence of supercritical water.

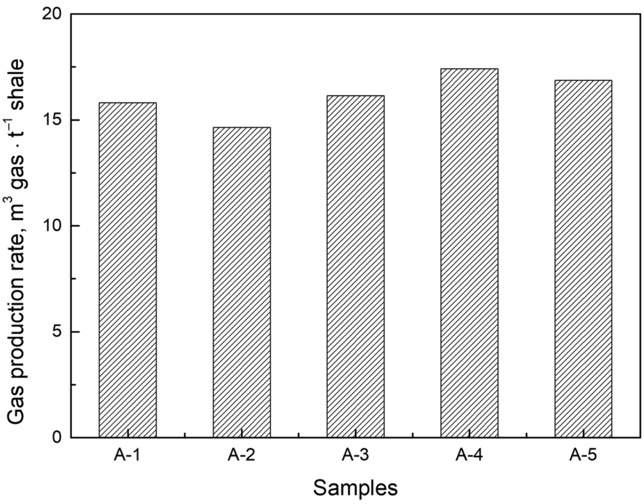

Fig. 4. Gas production rate of Maoming oil shale in the presence of supercritical water.

Table 3. Organic carbon content in wastewater

	A-1	A-2	A-3	A-4	A-5
TOC, mg/L	49.274	756.26	546.219	179.324	278.811

3.2.2. Product composition

Figure 5 presents the test results for the composition of oil-producing components, which includes gasoline, diesel, distillate, and heavy oil fractions. It is evident that the relative content of heavy oil distillate in the A-1 experiment was nearly zero, while the relative content of gasoline and distillate was considerably higher compared to the other four experiments. Although the relative content of diesel distillate in the A-1 experiment was slightly lower than in the other experiments, the total relative content of the three lighter components, excluding heavy oil distillate, decreased. This suggests that increasing the water-shale mass ratio enhances the conversion of heavy components into lighter ones during oil production.

Figure 6 depicts the carbon number distribution of oil production across the five experiments, revealing that the relative content of components below C20 in the A-1 experiment was significantly higher than in the other experiments. The findings from Figures 5 and 6 align, suggesting that increasing the water-shale mass ratio can enhance the quality of oil production and result in lighter oil.

Figure 7 illustrates the gas production composition across the five experiments, primarily consisting of hydrogen, methane, carbon dioxide, ethane, and carbon 3+ (C_{3+}) components. It is observed that the relative content of hydrogen and methane in the gas produced during the A-1 experiment was greater than in the other four experiments, indicating that a higher water-shale mass ratio may promote the production of hydrogen and methane.

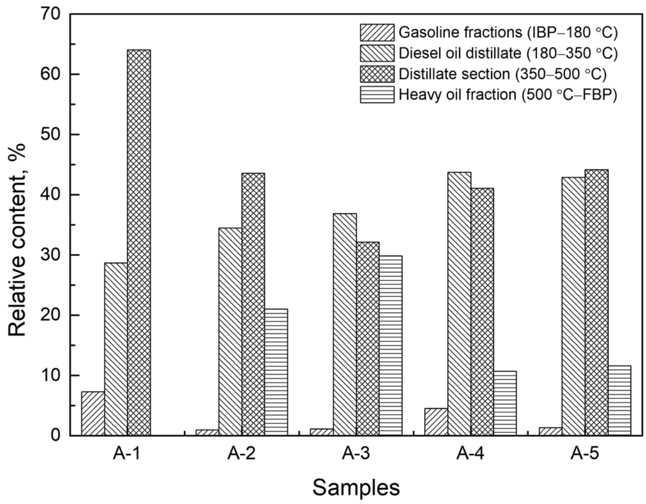

Fig. 5. Oil components in the presence of supercritical water. Abbreviations: IBP – initial boiling point, FBP – final boiling point.

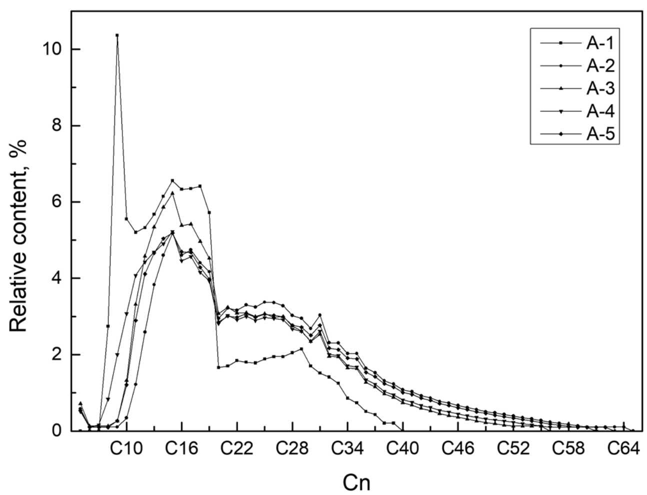

Fig. 6. Carbon number distribution of oil production in oil shale of Maoming Basin in the presence of supercritical water.

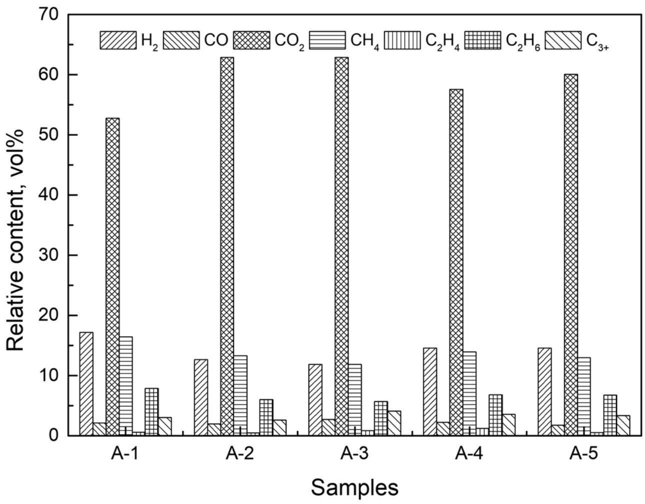

Fig. 7. Gas components in the presence of supercritical water.

4. Conclusions

In this paper, the hydrocarbon generation of Maoming oil shale was simulated in the presence of supercritical water using a visual self-developed reactor with high temperature and high pressure. The process of hydrocarbon generation was observed online. The effects of the water-shale mass ratio on hydrocarbon generation from Maoming oil shale were investigated. The following conclusions were drawn.

1. The critical temperature of oil generation can be effectively determined by pyrolysis experiments of oil shale through the visual reactor, which is a new method for determining the critical temperature of oil generation from oil shale. The critical temperatures of Maoming oil shale under supercritical water ranged from 262 to 292 °C. Using the visual reactor, convenient conditions are easily obtained for exploring the critical temperature of oil shale pyrolysis.
2. Maoming oil shale is highly heterogeneous, and the organic carbon conversion can reach more than 25.4% within the reaction time of 1 hour.
3. As the water-shale mass ratio increases, the conversion of organic carbon in oil shale and the production of shale oil are promoted, although no significant effects on gas production were found.
4. Increasing the water-shale mass ratio is beneficial for reducing the heavy oil fraction in oil production and promoting the selectivity of hydrogen and methane in gas production.

Data availability statement

The authors confirm that the data supporting the findings of this study are available within the article.

Acknowledgments

The financial support from the Basic Science Center Program of the Ordered Energy Conversion of the National Nature Science Foundation of China (No. 52488201) and the National Nature Science Foundation of China (No. 52376146) are gratefully acknowledged. The authors are thankful to the reviewers and editors for their work on this article. The publication costs of this article were partially covered by the Estonian Academy of Sciences.

References

1. Xie, T., Zhao, Q., Dong, Y., Jin, H., Wang, Y., Guo, L. Experimental investigation on the hydrocarbon generation of low maturity organic-rich shale in supercritical water. *Oil Shale*, 2022, **39**(3), 169–188. https://doi.org/10.3176/oil.2022.3.02
2. Kang, Z., Zhao, Y., Yang, D. Review of oil shale in-situ conversion technology. *Appl. Energy*, 2020, **269**, 115121. https://doi.org/10.1016/j.apenergy.2020.115121
3. Deng, S., Wang, Z., Gao, Y., Gu, Q., Cui, X., Wang, H. Sub-critical water extraction of bitumen from Huadian oil shale lumps. *J. Anal. Appl. Pyrolysis*, 2012, **98**, 151−158. https://doi.org/10.1016/j.jaap.2012.07.011
4. Akiya, N., Savage, P. E. Roles of water for chemical reactions in high-temperature water. *Chem. Rev.*, 2002, **102**(8), 2725−2750. https://doi.org/10.1021/cr000668w
5. Bake, K. D., Pomerantz, A. E. Optical analysis of pyrolysis products of Green River oil shale. *Energy Fuels*, 2017, **31**(12), 13345−13352. https://doi.org/10.1021/acs.energyfuels.7b01020
6. Tang, X., Li, S., Yue, C., He, J., Hou, J. Lumping kinetics of hydrodesulfurization and hydrodenitrogenation of the middle distillate from Chinese shale oil. *Oil Shale*, 2013, **30**(4), 517−535. http://dx.doi.org/10.3176/oil.2013.4.05
7. Lewan, M. Water as a source of hydrogen and oxygen in petroleum formation by hydrous pyrolysis. *Am. Chem. Soc., Div. Fuel Chem.*, 1992, **37**, 1643−1649.
8. Hou, L., Ma, W., Luo, X., Liu, J. Characteristics and quantitative models for hydrocarbon generation-retention-production of shale under ICP conditions: example from the Chang 7 member in the Ordos Basin. *Fuel*, 2020, **279**, 118497. https://doi.org/10.1016/j.fuel.2020.118497
9. Weingärtner, H., Franck, E. U. Supercritical water as a solvent. *Angew. Chem., Int. Ed.*, 2005, **44**(18), 2672−2692. https://doi.org/10.1002/anie.200462468
10. Zhao, Q., Guo, L., Huang, Z., Chen, L., Jin, H., Wang, Y. Experimental investigation on enhanced oil recovery of extra heavy oil by supercritical water flooding. *Energy Fuels*, 2018, **32**(2), 1685−1692. https://doi.org/10.1021/acs.energyfuels.7b03839

11. Guo, L., Jin, H., Lu, Y. Supercritical water gasification research and development in China. *J. Supercrit. Fluids*, 2015, **96**, 144−150. https://doi.org/10.1016/j.supflu.2014.09.023
12. Kruse, A. Supercritical water gasification. *Biofuels, Bioprod. Biorefin.*, 2008, **2**(5), 415−437. https://doi.org/10.1002/bbb.93
13. Reddy, S. N., Nanda, S., Dalai, A. K., Kozinski, J. A. Supercritical water gasification of biomass for hydrogen production. *Int. J. Hydrogen Energy*, 2014, **39**(13), 6912−6926. https://doi.org/10.1016/j.ijhydene.2014.02.125
14. Xie, T., Zhao, Q., Jin, H., Wang, Y., Guo, L. Reaction kinetics study on hydrocarbon generation of medium- and low-maturity organic-rich shale in supercritical water. *Energy Fuels*, 2023, **37**(18), 14192–14201. https://doi.org/10.1021/acs.energyfuels.3c02494
15. Xie, T., Zhao, Q., Jin, H., Wang, Y., Guo, L. Experimental investigation on the organic carbon migration path and pore evolution during co-thermal hydrocarbon generation of low maturity organic-rich shale and supercritical water. *Energy Fuels*, 2022, **36**(24), 15047–15054. https://doi.org/10.1021/acs.energyfuels.2c02932
16. Xie, T., Zhao, Q., Dong, Y., Jin, H., Wang, Y., Guo, L. Experimental investigation on hydrocarbon generation of organic-rich shale with low maturity in sub- and supercritical water. *Geoenergy Sci. Eng.*, 2023, **223**, 211553. https://doi.org/10.1016/j.geoen.2023.211553
17. Veski, R., Palu, V., Kruusement, K. Co-liquefaction of kukersite oil shale and pine wood in supercritical water. *Oil Shale*, 2006, **23**(3), 236−248. http://dx.doi.org/10.3176/oil.2006.3.04
18. Funazukuri, T., Yokoi, S., Wakao, N. Supercritical fluid extraction of Chinese Maoming oil shale with water and toluene. *Fuel*, 1988, **67**(1), 10–14. https://doi.org/10.1016/0016-2361(88)90004-X
19. Yanik, J., Yüksel, M., Sağlam, M., Olukçu, N., Bartle, K., Frere, B. Characterization of the oil fractions of shale oil obtained by pyrolysis and supercritical water extraction. *Fuel*, 1995, **74**(1), 46–50. https://doi.org/10.1016/0016-2361(94)P4329-Z
20. El Harfi, K., Bennouna, C., Mokhlisse, A., Ben chanâa, M., Lemée, L., Joffre, J., Amblès, A. Supercritical fluid extraction of Moroccan (Timahdit) oil shale with water. *J. Anal. Appl. Pyrolysis*, 1999, **50**(2), 163–174. https://doi.org/10.1016/S0165-2370(99)00028-5
21. Liang, X., Zhao, Q., Dong, Y., Guo, L., Jin, Z., Liu, Q. Experimental investigation on supercritical water gasification of organic-rich shale with low maturity for syngas production. *Energy Fuels*, 2021, **35**(9), 7657–7665. https://doi.org/10.1021/acs.energyfuels.0c04140
22. Hu, H., Zhang, J., Guo, S., Chen, G. Extraction of Huadian oil shale with water in sub- and supercritical states. *Fuel*, 1999, **78**(6), 645–651. https://doi.org/10.1016/S0016-2361(98)00199-9
23. Nasyrova, Z. R., Kayukova, G. P., Onishchenko, Y. V., Morozov, V. P., Vakhin, A. V. Conversion of high-carbon domanic shale in sub- and supercritical waters. *Energy Fuels*, 2020, **34**(2), 1329–1336. https://doi.org/10.1021/acs.energyfuels.9b03130